Influence of Heat Treatment on the Properties of Shape Memory Fibers. I. Crystallinity, Hydrogen Bonding, and Shape Memory Effect

Qinghao Meng, Jinlian Hu

Institute of Textiles and Clothing, The Hong Kong Polytechnic University, Hung Hom, Kowloon, Hong Kong, China

Received 9 August 2007; accepted 4 March 2008
DOI 10.1002/app.28363
Published online 9 May 2008 in Wiley InterScience (www.interscience.wiley.com).

ABSTRACT: Shape memory fibers (SMFs) were prepared via melt spinning. The fibers underwent different heat treatments to eliminate internal stress and structure deficiency caused during melt spinning. The influences of heat treatments on the SMF crystallinity, molecular orientation, hydrogen bonding, and shape memory behavior were studied. It was found with increasing heat-treatment temperature, the soft segment crystallinity, crystallite dimension, and microphase separation increased, and the hydrogen bonding in the hard segment phase increased. Low temperature heat treatments decreased the shape recovery ratios while increasing the shape fixity ratios as a result of internal stress releasing and molecules disorientation. High temperature heat treatments increased the hard segment stability. Increasing heat-treatment temperature resulted in the improvement of both the shape recovery and fixity, because it promoted the phase separation. The results from DSC, DMA, XRD, and FTIR were used to illustrate the mechanism governing these properties difference. © 2008 Wiley Periodicals, Inc. J Appl Polym Sci 109: 2616–2623, 2008

Key words: polyurethanes; stimuli–sensitive polymers

INTRODUCTION

The thermally active shape memory fiber (SMF) is one smart material, which can fix temporary elongation at a temperature below the switching temperature and recover the original length when heated to a temperature above the switching temperature.[1–10] The most immediate application area of the SMF is in textile and clothing industry, because it can provide inspiration to create intelligent textiles with a self-regulating structure and performance in response to external stimulus.[11,12]

Similar to the shape memory effect of shape memory films, the shape memory effect of shape memory polyurethane fibers is also due to the phase separation of the hard segments (aromatic diisocyanates and small size diols or diamines) and soft segments (aliphatic polyether or polyester) in the polyurethane molecules.[13–19] The aggregated hard segment phase, which has a higher thermal transition temperature acting as the physical crosslinking, is in charge of memorizing original shape while the soft phase, which has a low transition temperature T_m or T_g (switching transition temperature) acting as a ''switch'' is responsible for fixing the temporary shape. If the shape memory fibers are stretched at a temperature above or below (cold draw) the switching temperature, the deformation can be fixed at the temperature below the switching temperature. Indispensably, they can recover to the original length upon heating to be above the switching temperature.[20–24]

Among the SMF spinning methods, (i) dry, (ii) wet, (iii) chemical, and (iv) melt spinning,[5,25] the melt spinning is the most advantageous in terms of health, safety, environmental protection, and economy concerns, because it does not involve the use of organic solvents.[7] In this study, the SMFs were fabricated by melt spinning. Heat treatments were applied to the fiber to eliminate internal stress and structure deficiency. The influences of heat treatments on the fiber thermal properties, crystalline properties, molecules orientation, hydrogen bonding, and shape memory behavior were studied.

EXPERIMENTAL

Materials

The shape memory polyurethane based on polyester polyol was obtained from shape memory textiles research center at the Hong Kong Polytechnic University. It is a PCL-4000-based shape memory polyurethane.[2,4–6] The soft segment phase has a glass

Correspondence to: J. Hu (tchujl@inet.polyu.edu.hk).
Contract grant sponsor: High-Performance Advanced Materials for Textile and Apparel (Project).
Contract grant sponsor: Hong Kong Innovation Technology; contract grant number: GHS/088/04.

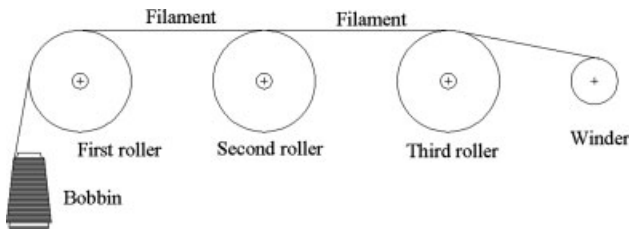

Figure 1 The schematic presentation of the heat treatment.

transition at about −50°C and a melting transition at about 47°C.

Melt spinning

The shape memory polyurethane fibers were spun using a laboratory-spinning machine with highly pure nitrogen protection. Spinning temperature was 210°C; winding up speed 100 m/min. The prepared SMFs were 70 dtex in linear density. The fiber's soft segment phase was a partially crystalline phase, and the melting transition temperature was the switching transition temperature of the SMFs.[23,26,27] The filament surface image of the SMF was taken using a Leica Stereoscan 440 scanning electron microscope. The operating voltage was 20 kV.

Heat treatment

The SMFs underwent heat treatments on a three-roller drawing unit (Alex James and Associate). The schematic representation of the heat treatment process is shown in Figure 1. The speed of the three rollers was 40 m/min. The temperature of the three rollers was same. At last, the filaments were wound up at relaxation state without external stress. The specimens were donated as SMF-X°C, that is, SMF-65°C, SMF-85°C, SMF-105°C, and SMF-125°C, where the X was the heat treatment temperature. After the heat treatments, the fibers were stored in a constant temperature and humidity laboratory (temperature: 22°C, relative humidity: 61%) for 7 days before property characterizations.

Differential scanning calorimeter analyses

The thermal properties of the as-spun fiber and SMFs after heat treatment were investigated through a differential scanning calorimeter (DSC) (PerkinElmer Diamond) with nitrogen as purge gas. Indium and zinc were used for calibration. Samples were washed with methanol to remove the oil and air dried before testing. The samples were first cooled from ambient temperature to −70°C at a cooling rate of 20°C/min. Then the fibers were reheated to 250°C at a heating rate of 10°C/min to investigate the thermal properties.

Dynamic mechanical analysis

Dynamic mechanical analysis (DMA) tests were carried out on a PerkinElmer Diamond Dynamic Mechanical Analyzer operated in a tensile mode. The heating rate was 2°C/min, testing frequency 2 Hz, and the oscillation amplitude 5.0 μm. Tests were conducted over the temperature range from −120 to 250°C. The gauge length between the clamps was 15 mm. The fiber cross-sectional area was measured from the cross-sectional photos taken by an optical microscope (×400 times).

X-ray diffraction analyses

The X-ray diffraction analyses (XRD) data were recorded by using a Philips analytical X-ray (Philips Xpert XRD System) at a voltage of 40 V, 30 mA current with a radiation wavelength of 1.542 Å. Spectra were obtained in a range of Bragg's angle $2\theta = 15°–45°$ with scanning step size 0.02° and time per step 1 s.

Sonic modulus

The sonic velocities and sonic modulus of the SMFs after heat treatment at different temperature were measured by using the SCY-111 sonic velocity apparatus (Donghua University of China). The tests are based on the presumption that sonic waves can travel faster if the orientation of fibers increases.

Fourier Transform Infrared spectrometry

The SMF IR transmission spectra were determined using a PerkinElmer (2000 FTIR) spectrometer in the region of 700–4000 cm^{-1} at room temperature. The SMFs were cut into small sects to make KBr tablets. Each sample was scanned 30 times at a resolution of 2 cm^{-1} and the scan signals were averaged. To make a comparison, all IR spectra were normalized by using the height of the 1412 cm^{-1} peak, assigned to the C—C stretching mode of the aromatic ring.[28–30]

Thermomechanical cyclic tensile investigations

Thermomechanical cyclic tensile tests were carried out by using the Instron 4466 equipped with a temperature controlled chamber. In the measurement, the fiber has a gauge length ~ 20 mm. The thermomechanical cyclic tensile test consists of five steps. The programmed testing path is shown in Figure 2.[3] (1) First, the fiber was heated to 70°C (T_{high}) and stretched to 100% strain at a speed of 10 mm/min at

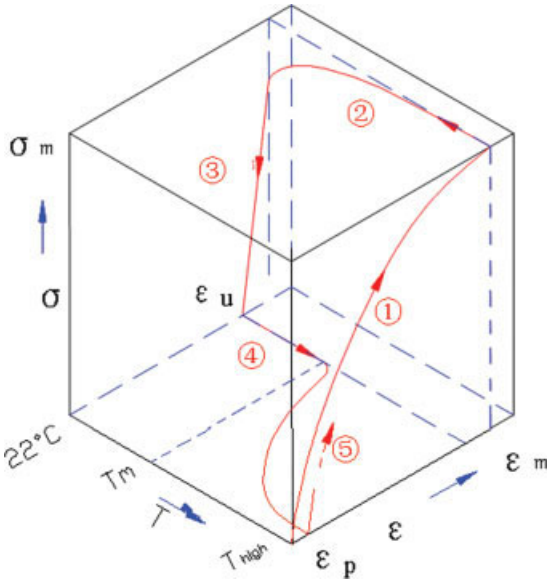

Figure 2 The schematic representation of the cyclic tensile testing path. [Color figure can be viewed in the online issue, which is available at www.interscience.wiley.com.]

this temperature; (2) then the fiber was cooled to ambient temperature (22°C) and the 100% strain was kept for 15 min; (3) the clamp was unloaded, and the fiber was allowed returning to the original position at a speed of 40 mm/min; (4) the fiber was then heated to 70°C; (5) procedure (1–4) was repeated. The above cycle was repeated four times on each fiber. In Figure 2, ε_m is the defined maximum strain in the cyclic tensile tests. In this study, ε_m is 100%. ε_u is the strain after unloading at ambient temperature (22°C) and $\varepsilon_p(N)$ is the residual strain after recovery in the Nth cycle. The fixity ratio (R_f) and recovery ratio (R_r) after the Nth cycle are calculated according to following equations[3]:

$$R_f(N) = \varepsilon_u(N)$$

$$R_r = (1 - \varepsilon_p(N)) \times 100\%$$

RESULTS AND DISCUSSION

DSC analyses

The surface image of the prepared SMFs are shown in Figure 3. The SMFs have a smooth surface.

The DSC thermograms of PCL-4000, as-spun SMF, and SMFs after heat treatment are presented in Figure 4, and the thermal property parameters are tabulated in Table I. The soft segment crystallinity was calculated from the enthalpy data ΔH of the crystallization by using the 140 J/g enthalpy value for fusion of 100% crystalline PCL given by Crescenzi et al.[28,31]

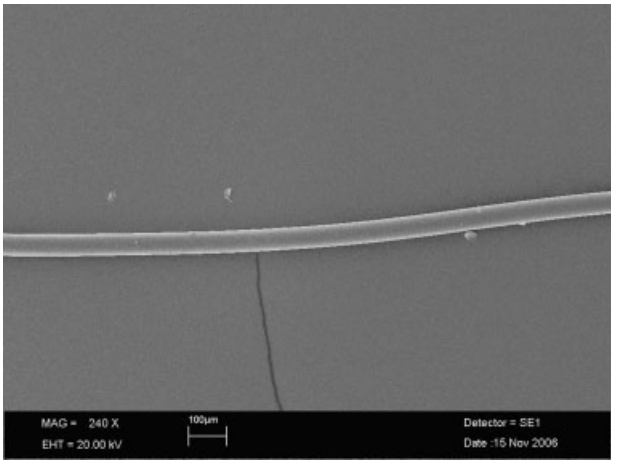

Figure 3 The surface image of the prepared SMFs.

In the as-spun SMF DSC curve, the melting transition peak in the vicinity of 41°C is ascribed to the soft segment melting transition.[22,23] Because of the impendence of the hard segment, the crystallinity of soft segment PCL decreases and the melting transition temperature decreases simultaneously in comparison with that of pure PCL. From Figure 4 and Table I, it can be seen that the heat treatment has a remarkable influence on the soft segment phase crystallization of the SMFs. With increasing heat treatment temperature, the soft-segment crystallinity increases from 18.8% of as-spun SMF to 28.4% of SMF-125°C. The melting transition temperature increases from 41.20°C to 48.58°C.

The heat treatment, especially high-temperature heat treatment, also has an influence on the SMFs hard segment phase. It seems that low-temperature heat treatment nearly has no influence on the hard segment phase. However, after 125°C heat treatment,

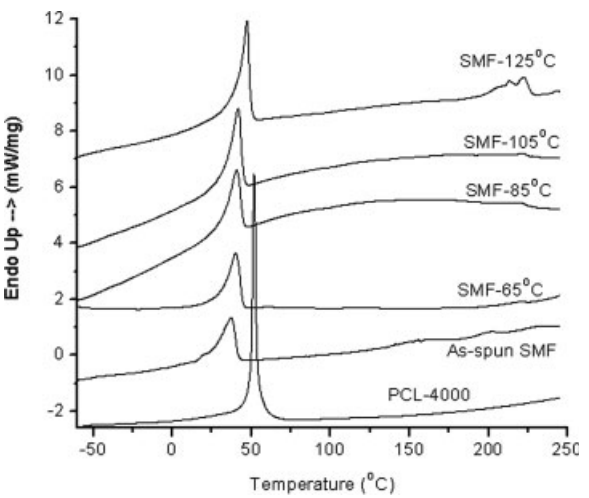

Figure 4 DSC thermograms of as as-spun SMF and SMFs after heat treatment.

TABLE I
Thermal Properties of As-Spun SMF and SMFs After Heat Treatment (T_m is Crystal Melting Temperature, ΔH the Heat of Fusion)

	Soft Segment		
	T_m (°C)	ΔH (J/g)	Crystallinity (%)
PCL-4000	59.00	53.68	39.8
SMF-125°C	48.58	38.36	28.4
SMF-105°C	46.46	36.85	27.3
SMF-85°C	45.35	34.97	25.9
SMF-65°C	43.64	31.68	23.5
As-spun SMF	41.20	25.34	18.8

the SMF shows obvious hard segment endothermic peaks, which appear to be related to the relatively short-range-ordered hard segments. According to the previous studies,[32,33] the glass transition temperature of the hard segment in polyurethane is located at around 125°C, and the melting point of hard segment phase crystals is in the range of 200–240°C.[34] The above results suggest the high-temperature heat treatment benefits for the hard segment aggregation to form stable hard segment phase.

DMA analysis

The dynamic mechanical properties of SMF-125°C, which had the highest dimensional stability, were evaluated. Because of the severe shrinking of the other fibers with increasing temperature, the dynamic mechanical properties of the as-spun SMF and SMF-65°C, SMF-85°C, and SMF-105°C cannot be tested. The elastic modulus (E') and loss tangent (tan δ) of the SMF-125°C over the temperature range from −110 to 190°C are presented in Figure 5. The E' of the SMF-125°C shows a sharp drop at about −50°C and a second sharp drop at 47°C. The loss tangent reflects the strain energy dissipated by viscous friction. According to the dependence of loss tangent on temperature, the peak locating at −50°C belongs to the glass transition temperature of the soft segment phase; the sharp increase at 47°C is attributed to the melting transition of soft segment phase.[35,36] This result is consistent with the DSC results. At a temperature above soft segments melting transition, the mechanical properties of the polyurethane is almost completely contributed by the hard segments phase[37] as can be seen by the plateau region of E'. This also proves the existence of the hard segment rich phase.[36] Upon heating above 175°C, another sharp decrease of E' is observed, indicating that the physical crosslinking cites between hard segments are totally destroyed.

The shape memory effect of the SMFs can be illustrated using the DSC and DMA results. When the fibers are heated to 70°C, which is above the soft

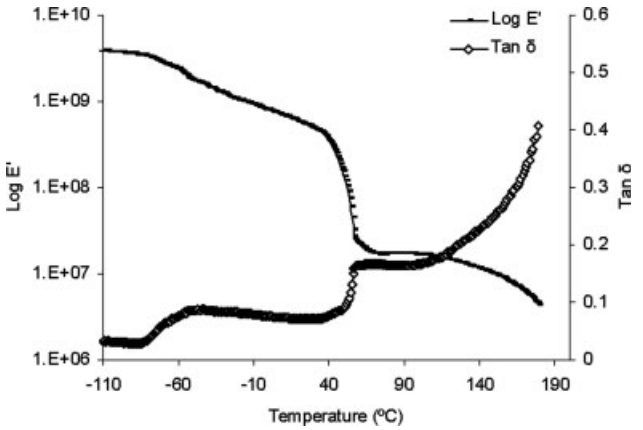

Figure 5 The elastic modulus and loss tangent of the SMF-125°C.

segment phase melting transition temperature (T_{trans}), the soft segments are in a random state. If they are stretched, the soft segments are extended. Once the temperature is cooled to below T_{trans}, the soft segments crystallize. As a result, the internal stress is stored in the fibers (mostly between the hard segments) and an associated deformation is fixed temporally. If they are reheated to above T_{trans}, the soft segments become flexible and the fibers resume to the folded configuration because of the release of internal stress stored between the hard segments. As a result, the fibers recover to their original length.

XRD analysis

The crystalline structures and unit cell parameters of pure PCL-4000, as-spun SMF, and SMFs after heat treatment at different temperature were studied using XRD. The patterns are shown in Figure 6, and the obtained results of lattice parameters are tabulated in Table II. The percent crystallinity (X_c) within

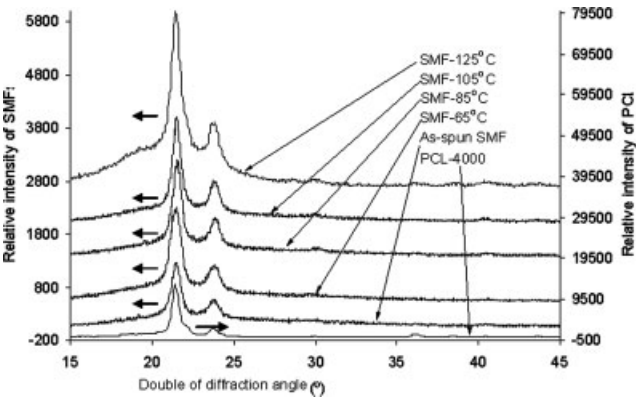

Figure 6 Wide-angle X-ray scattering patterns of as-spun SMF and SMFs after heat treatment.

TABLE II
The Results of Peak Separation and Calculated Crystallinity

Sample		Peak position 2θ (°)	FWHM (°)	Height (count)	Area (count)	Crystallinity (%)
PCL-4000	1	20.61	7.07	732.7	6298.1	
	2	21.43	0.44	9280.8	5001.1	
	3	22.11	0.37	1171.2	552.7	
	4	23.78	0.55	959.9	640.1	
	5	29.92	1.27	126.1	194.3	
	6	36.15	0.53	591.9	383.0	
	7	38.45	0.39	198.5	94.8	
	8	41.10	17.04	162.6	3367.8	41.53
As-spun SMF	1	21.44	7.19	77.1	6731.6	
	2	21.45	0.7	2297.6	1840.2	
	3	23.87	0.82	666.0	545.3	
	4	28.62	0.58	55.9	39.2	
	5	29.97	1.07	78.1	101.2	
	6	40.33	19.43	93.7	2212.4	22.02
SMF-65°C	1	21.43	6.48	1460.2	1118.9	
	2	21.47	0.66	738.5	517.0	
	3	23.84	0.73	264.7	185.4	
	4	28.39	13.60	1315.3	1106.7	
	5	29.87	0.75	20.7	14.5	
	6	40.50	0.81	21.9	15.4	24.76
SMF-85°C	1	21.21	6.30	191.5	1465.8	
	2	21.48	0.63	1145.0	773.8	
	3	23.81	0.67	372.9	289.9	
	4	27.18	16.75	75.1	1527.7	
	5	29.96	0.47	42.2	24.2	
	6	40.46	0.71	35.2	24.7	27.10
SMF-105°C	1	21.17	6.02	175.0	1280.3	
	2	21.5	0.56	1072.1	746.5	
	3	23.8	0.66	343.5	274.6	
	4	27.27	14.53	73.2	1292.1	
	5	30.08	0.74	29.1	26.2	
	6	40.63	1.35	19.5	31.9	29.55
SMF-125°C	1	20.77	6.49	198.9	1569.7	
	2	21.54	0.54	1034.7	873.4	
	3	23.78	0.64	303.4	300.6	
	4	27.88	14.35	62.7	1092.5	
	5	29.89	1.06	16.7	21.6	
	6	40.54	0.73	14.5	12.9	31.22

the sample was calculated using the method described by Young and Lovell.[38]

$$Xc = \left(\frac{\sum_i A_{ci}}{\sum_i A_{ci} + \sum_j A_{Aj}} \right) \times 100\%$$

where the A_c is the area of the X-ray diffraction curve due to scattering from the crystalline phase and A_a is the area of the X-ray diffraction curve due to scattering from amorphous.

The average crystallite size was determined coarsely using Debye-Scherrer formula[39,40]: $L_{(hkl)} = k\lambda/\beta \cos \theta$. Here, λ is the applied X-ray wave length $\lambda_{Cu} = 1.542$ Å; θ is diffraction angle, $k = 0.89$, β-FWHM (full width at half maximum) in radians.

Contrary to the DSC curve of SMF-125°C where a melting endothermic peak appears during the SMF heating scanning, no obvious hard segment crystal diffraction peak is observed in the XRD curve of SMF-125°C. This may be because in the SMF the hard segments is relatively short-range ordered and not well-ordered enough to form crystallites.

The peaks of XRD curves were separated and areas of the X-ray scattering of every amorphous phase broad peak and sharp crystalline phase peak were integrated using the Philips Xpert XRD system soft ware. The peaks separating results and calculated crystallinities are presented in Table II. The crystallinities changing trend with increasing heat treatment temperature are generally consistent with those obtained from DSC analysis. The heat treatment increases the crystallinity and as a result benefits the phase separation.[22]

The influence of heat treatments on the unit cell parameters was also studied. From Figure 6, it can see that all the PCL-4000, as-spun SMF, and SMFs

TABLE III
The Lattice Parameters of the SMFs

	(110)			(200)		
Sample	2θ	FWHM (°)	$L_{(hkl)}$	2θ	FWHM (°)	$L_{(hkl)}$
PCL-4000	21.43	0.44	181.64	23.78	0.55	145.91
As-spun SMF	21.45	0.7	114.18	23.87	0.82	97.88
SMF-65°C	21.47	0.66	121.10	23.84	0.73	109.95
SMF-85°C	21.48	0.63	126.87	23.81	0.67	119.78
SMF-105°C	21.5	0.56	142.74	23.8	0.66	121.60
SMF-125°C	21.54	0.54	148.03	23.78	0.64	125.39

after heat treatment have two prominent diffraction peaks at about 21.5° and 23.80°, respectively. The peak at 21.5° can be attributed to the (110) plane diffraction of PCL soft segment. The peak at 23.80° occurs due to the (200) plane diffraction.[41] The unit cell parameters of the PCL and SMFs are presented in Table III.

For (110) plane, with an increasing heat-treatment temperature, the average crystallite size increases. For (220), with increasing heat-treatment temperature, the average crystallite size also increases. Generally, the heat treatment increases the soft segment crystallites dimension.

Sonic modulus

The sonic velocities *C* and sonic modulus *E* of the SMFs before and after heat treatment at different temperature are shown in Figure 7. To make a comparison, the as-spun fiber is designated as the SMF after heat treatment at ambient temperature (22°C). For the SMFs under study, the sonic modulus decreases significantly at low temperature heat treatment. This is because the SMFs have a melting transition at a low temperature. During the low-temperature heat treatment, the internal stress stored among the hard segment phase during the spinning process release accompanied with soft segment disorientation. Continuously, increasing heat-treatment temperature has no obvious influence on the SMFs sonic modulus.

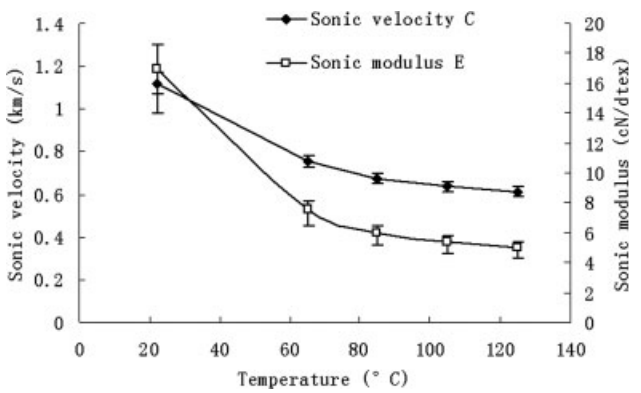

Figure 7 The sonic velocity *C* and sonic modulus *E* of the as-spun fiber and SMFs after different temperature heat treatment.

Hydrogen-bonding analysis

It has been well known that the hydrogen bonding between functional groups of polyurethanes has remarkably influences on polyurethane properties.[28,42–46] To study the hydrogen bonding of polyurethanes, the carbonyl stretching bands is mostly used because the quantitative results based on *N*—H bands are not reliable considering amido conformation change.[28,43,47] In addition, the mole absorptive ratio of hydrogen boned amido and free amido was 4.6 : 1, while that of carbonyl group is 1.05 : 1. So it is more convenient to use the carbonyl group to study the hydrogen bonding even though the hard segment amide band composes the complete hydrogen bonding.[28,43,48]

In this study, to make a comparison, the FTIR spectra of pure PCL-4000, as-spun SMF, and SMFs after heat treatment from 1800 to 1550 cm^{-1} are tested, and the results are shown in given in Figure 8. For the pure PCL, where no hydrogen-bonded

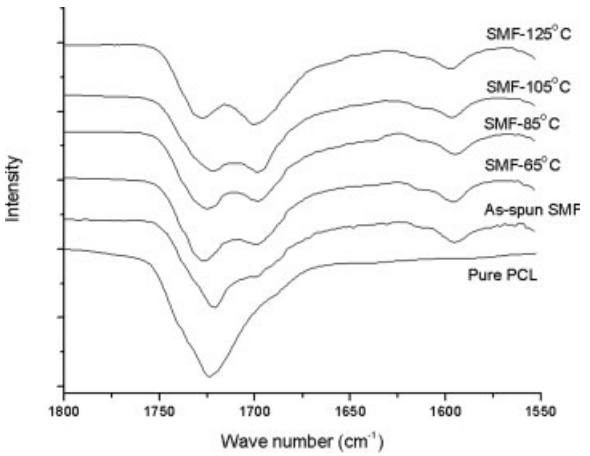

Figure 8 Carbonyl absorption in the FTIR spectra of pure PCL-4000 and SMFs as the function of increasing heat-treatment temperature.

carbonyl group exists, the carbonyl group stretching vibration displays the absorption peak at 1723 cm^{-1}. In the SMFs, the free carbonyl group peak locates at about 1728 cm^{-1} and hydrogen-bond carbonyl group peak situates at 1701 cm^{-1}.[49] It can be seen that with increasing heat-treatment temperature, the peak intensity of the free carbonyl group decreases and the area of free carbonyl group peak reduces. Simultaneously, the peak intensity of the hydrogen-bonded carbonyl group increases, and the corresponding area increases with increasing heat treatment temperature. These suggest that with increasing heat treatment temperature, part of the free carbonyl groups transform to hydrogen-boned groups.

In fact, in the SMFs, two kinds of hydrogen bonding of carbonyl groups coexist. One is the hydrogen bonding in the hard segments phase between carbonyl group and hydrogen of amido. Another is the hydrogen bonding between carbonyl group in the soft segment and hydrogen of amido in the hard segment. According to the previous studies [28–30,46], the wave number difference of these two hydrogen bondings is generally so small that they are difficult to separate in the IR spectra.[30,42,50] According to the results obtained from DSC and XRD analysis, the heat treatment increases the crystallinity and ''purity'' of soft segment phase, as a result, the hydrogen bonding between carbonyl group in the PCL soft segment and hydrogen of amido in the hard segment decreases.[15,28,43] So, it can be concluded that the hydrogen bonding in the hard segment phase increases. This result also indicates that a more stable hard segment phase is formed in the SMF after heat treatment.

Shape memory effect

The shape fixity ratios and recovery ratios of the as-spun SMF and SMFs after heat treatment are shown in Figures 9 and 10. After 65°C heat treatment, the recovery ratios of the SMF decrease remarkably,

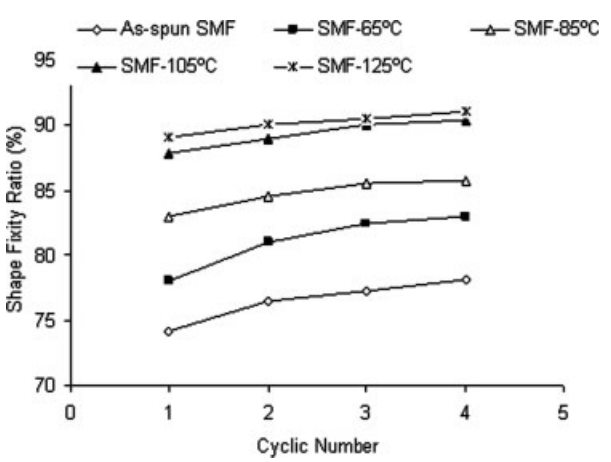

Figure 9 Shape memory recovery ratios of SMFs.

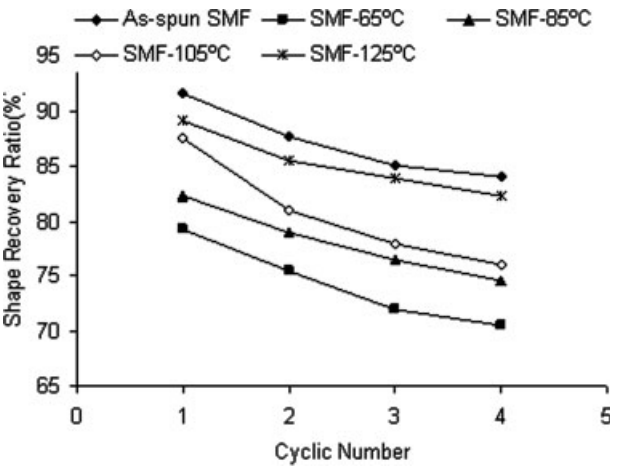

Figure 10 Shape fixity ratios of SMFs.

while the fixity ratios increase. With increasing heat-treatment temperature, both the shape recovery ratios and fixity ratios increase.

The shape memory effect changes after heat treatments can be interpreted as follows. In polyurethane bulk systems, the soft segment phase is in charge of shape fixity by freezing the polyurethane molecules after being cooled to a temperature below the switching transition temperature, and the hard segment phase acting as physical crosslinking is responsible for shape recovery by releasing the stress stored during deformation.[22,24,26,51] However, for the SMFs which have molecular orientation and internal stress caused during melt spinning, the fiber will shrink because of the stress released and molecules disorientation. So after 65°C heat treatment, the recovery ratios decrease and fixity ratios increase. With increasing heat-treatment temperature, as established earlier, the soft segment phase crystallinity and phase separation increase. The hard segment phase stability improved especially after 125°C heat treatment. So, the soft segment has more capacity to freeze the polyurethane molecules when the fiber is cooled from temperature above the switching transition temperature to the ambient temperature. In addition, a more stable hydrogen-bonded hard segment network is produced after the heat treatment, so that more deformation energy can be stored in the hard segment phase. And consequently the SMF has more power to recover to the original length when it is heated to a temperature above the switching transition temperature. As a whole, the shape fixity ratios and recovery ratios increase with increasing heat-treatment temperature.[5,6]

CONCLUSIONS

In this work, shape memory fibers were prepared using melt spinning. The fibers were subjected to

different heat treatments to eliminate internal stress and structure deficiency caused during the melt-spinning process. The influences of heat-treatment temperature on the SMF crystallinity, molecular orientation, hydrogen bonding, and shape memory behavior were studied using DSC, DMA, XRD, sonic velocity apparatus, and FTIR and thermomechanical cyclic tensile testing. It was found with increasing heat-treatment temperature, the soft segment crystallinity, crystallite, and microphase separation increased. The hard segment stability increased especially by high-temperature heat treatment. The low-temperature heat treatment decreased the shape recovery ratios while increased the shape fixity ratios because of internal stress releasing and molecules disorientation. Increasing heat-treatment temperature increased both the shape recovery ratio and fixity ratio, because the heat treatment increased both the soft segment phase crystallinity and hard segment phase stability.

References

1. Hayashi, S.; Tasaka, Y.; Hayashi, N.; Akita, Y. Tech Rev 2004, 41, 1.
2. Ji, F. L.; Zhu, Y.; Hu, J. L.; Liu, Y.; Yeung, L. Y.; Ye, G. D. Smart Mater Struct 2006, 15, 1547.
3. Lendlein, A.; Kelch, S. Angew Chem Int Ed 2002, 41, 2034.
4. Zhu, Y.; Hu, J. L.; Yeung, L. Y.; Liu, Y.; Ji, F. L.; Yeung, K. W. Smart Mater Struct 2006, 15, 1385.
5. Zhu, Y.; Hu, J. L.; Yeung, L. Y.; Lu, J.; Meng, Q. H.; Chen, S. J.; Yeung, K. W. Smart Mater Struct 2007, 16, 969.
6. Meng, Q. H.; Hu, J. L.; Zhu, Y.; Lu, J.; Liu, Y. Smart Mater Struct 2007, 16, 1192.
7. Meng, Q. H.; Hu, J. L.; Zhu, Y. J Appl Polym Sci 2007, 106, 837.
8. Meng, Q. H.; Hu, J. L. Polym Adv Technol 2008, 9, 31.
9. Meng, Q. H.; Hu, J. L.; Mondal S. DOI 10.1016/j.memsci. 2008.03.032. J Membr Sci, 2008.
10. Meng, Q. H.; Hu, J. L.; Zhu, Y.; Lu, J.; Liu, Y. J Appl Polym Sci 2007, 106, 2515.
11. Tang, S. L. P.; Stylios, G. K. Int J Cloth Sci Technol 2006, 18, 108.
12. Liu, Y.; Chung, A.; Hu, J. L.; Lu, J. J Zhejiang Univ Sci A 2007, 8, 830.
13. Mondal, S.; Hu, J. L. Carbohydr Polym 2007, 67, 282.
14. Zhu, Y.; Hu, J. L.; Yeung, K. W.; Liu, Y. Q.; Liem, H. M. J Appl Polym Sci 2006, 100, 4603.
15. Zhu, Y.; Hu, J. L.; Yeung, K. W.; Fan, H. J.; Liu, Y. Q. Chin J Polym Sci 2006, 24, 173.
16. Lendlein, A.; Langer, R. Science 2002, 96, 1673.
17. Zhang, Z. R. Shape Memory Bone Fixing Splint in China Pat CN20020150720, 2004.
18. Hu, J. L.; Ding, X. M.; Tao, X. M. J China Text Univ 2002, 19, 89.
19. Ciardelli, G.; Rechichi, A.; Sartori, S.; Acunto, M. D.; Caporale, A.; Peggion, E.; Vozzi, G.; Giusti, P. Polym Adv Technol 2006, 17, 786.
20. Yoshihaya, N.; Ishihara, H.; Yamada, T. Polym Eng Sci 2003, 43, 1740.
21. Fourne, F. Synthetic Fibers Machines and Equipment, Manufacture, Properties; Hanser: Munich, 1999.
22. Lin, J. R.; Chen, L. W. J Appl Polym Sci 1998, 69, 1563.
23. Lin, J. R.; Chen, L. W. J Appl Polym Sci 1998, 69, 1575.
24. Kim, B. K.; Lee, S. Y. Polymer 1998, 39, 2803.
25. Hu, J. L.; Meng, Q. H.; Zhu, Y.; Lu, J.; Zhuo, H. T. (October 6 2007) Shape Memory Fibers Prepared by Wet, Reaction, Dry, Melt, and Electro Spinning in US Pat 11/907,012.
26. Tobushi, H.; Hashimoto, T.; Ito, N.; Hayashi, S.; Yamada, E. J Intell Mater Syst Struct 1998, 9, 127.
27. Takahashi, T.; Hayashi, N.; Hayashi, S. J Appl Polym Sci 1998, 60, 1061.
28. Luo, N.; Wang, D. N.; Ying, S. K. Polymer 1996, 37, 3577.
29. Seymour, R. W., Jr.; Allegrezza, A. E.; Cooper, S. L. Macromolecules 1973, 6, 896.
30. Luo, N.; Wang, D. N.; Ying, S. K. Macromolecules 1997, 30, 4405.
31. Crescenzi, V.; Manzini, G.; Calzolari, G.; Borri, C. Eur Polym J 1972, 8, 449.
32. Seefried, C. G., Jr.; Koleske, J. V.; Critchfield, F. E. J Appl Polym Sci 1975, 19, 2503.
33. Seefried, C. G., Jr.; Koleske, J. V.; Critchfield, F. E. J Appl Polym Sci 1975, 19, 2493.
34. Briber, R. M.; Thomas, E. L. J Macromol Sci Phys 1983, 22, 509.
35. Kim, B. K.; Lee, S. Y.; Xu, M. Polymer 1996, 37, 5781.
36. Chen, S. A.; Chan, W. C. Polym Phys 2003, 28, 1499.
37. LaShanda, T.; Jams Korley, B. D. P.; Thomas, E. L.; Hammond, P. T. Polymer 2006, 47, 3073.
38. Young, R. J.; Lovell, P. A. Introduction to Polymers, 2nd ed.; Chapman & Hall: London, 1991.
39. Patterson, A. L. Phys Rev 1939, 56, 978.
40. Mo, Z.; Lee, K.; Moon, Y. B.; Kobayashi, M.; Heeger, A. J.; Wudl, F. Macromolecules 1985, 18, 1972.
41. Marchessault, R. H.; Bittiger, H. Acta Crystallogr B 1970, 26, 1923.
42. Coleman, M. M.; Lee, K. H.; Skrovanek, D. J.; Painter, P. C. Macromolecules 1986, 19, 2149.
43. Coleman, M. M.; Skrovanek, D. J.; Hu, J. B.; Painter, P. C. Macromolecules 1988, 21, 59.
44. Lee, H. S.; Wang, Y. K.; Hsu, S. L. Macromolecules 1987, 20, 2089.
45. Chu, B.; Gao, T.; Li, Y. J.; Wang, J.; Desper, C. R.; Catherine, A. B. Macromolecules 1992, 25, 5724.
46. Sung, C. S. P.; Schneider, N. S. Macromolecules 1977, 10, 452.
47. Frisch, K. C.; Reegen, S. L. Adv Urethane Sci Technol 1978, 6, 1.
48. Senich, G. A.; MacKnight, W. J. Macromolecules 1980, 13, 106.
49. Xiao, F. F.; Shen, D. Y.; Zhang, X.; Hu, S. R.; Xu, M. Polymer 1987, 28, 2335.
50. Harthcock, M. A. Polymer 1989, 30, 1234.
51. Li, F. K.; Zhang, X.; Hou, J. A.; Xu, M.; Luo, X. L.; Ma, D. Z.; Kim, B. K. J Appl Polym Sci 1996, 64, 1511.